

*Regular article***Phase change problems with free convection: fixed grid numerical simulation**Marilena Giangi<sup>1</sup>, Fulvio Stella<sup>1</sup>, Tomasz A. Kowalewski<sup>2</sup><sup>1</sup> Univ. di Roma "La Sapienza", Via Eudossiana 18, I-00184 Rome, Italy<sup>2</sup> IPPT-PAN, Polish Academy of Science, PL 00-049 Warsaw, Poland

Received: 30 April 1999 / Accepted: 17 June 1999

Communicated by: M. Espedal and A. Quarteroni

**Abstract.** A numerical and experimental study of unsteady natural convection during freezing of water is presented. The mathematical model for the numerical simulations is based on the enthalpy-porosity method in vorticity-velocity formulation, equations are discretised on a fixed grid by means of a finite volume technique. A fully implicit method has been adopted for the mass and momentum equations. Experiments are performed for water in a differentially heated cube surrounded by air. The experimental data for natural convection with freezing in the cavity are collected to create a reference for comparison with numerical results. The method of simultaneous measurement of the flow and temperature fields using liquid crystal tracers is used. It allows us to collect transient data on the interface position, and the temperature and velocity fields. In order to improve the capability of the numerical method to predict experimental results, a conjugate heat transfer problem was solved, with finite thickness and internal heat conductivity of the non-isothermal walls. These results have been compared with the simulations obtained for the idealised case of perfectly adiabatic side walls, and with our experimental findings. Results obtained for the improved numerical model shown a very good agreement with the experimental data only for pure convection and initial time of freezing process. As time passes the discrepancies between numerical predictions and the experiment became more significant, suggesting a necessity for further improvements of the physical model used for freezing water.

formed and the convective flow in the melt. Proper modelling of the flow problems becomes necessary for controlling fundamental parameters of the technological applications like casting, welding, soldering, and processing of alloys or crystal growth at low gravity environment. Due to the problem complexity, direct application of numerical methods to the engineering problem of solidification is not a trivial task. Errors appear due to limited accuracy of different numerical methodologies (eg. adaptive grid by Yeoh et al. 1990 [1], fixed grid FEM by Banaszek et al. 1998 [2], fixed grid FDM by Giangi et al. 1998 [3]), and due to inevitable simplifications introduced in the models. Our previous numerical attempts appear to fail in modelling the details of the water solidification. The numerical simulations performed by Kowalewski and Rebow (1998) [4] or Giangi et al. (1998) [3] show several differences in the front shape and flow pattern. It seems that the numerical models used need several improvements. In the present paper we verified several assumptions made in the modelling. The effect of finite conductivity of both non-isothermal and isothermal walls is also discussed. The experimental verification of numerical models has special importance for phase change problems. However, the available comparisons with experiment appear to be insufficient. This is, perhaps, due to the fact that most of the accessible experimental data on freezing are limited to general observations of the phase change front and point measurements of the flow velocity and temperature. Hence, the primary target of the experimental part is to create a physical benchmark for the problem of natural convection in freezing water under free surface conditions. To avoid geometrical complications and uncertainty of the thermophysical properties, a simple model of water freezing in a differentially heated cavity will be used for code testing purposes. The experimental data on freezing of water in the cube-shaped cavity are collected to create a reference for comparison with numerical results. The method of simultaneous measurement of the flow and temperature fields using liquid crystal tracers is used. It allows us to collect transient data on the interface position, and the temperature and velocity fields [5].

In this paper our numerical model is verified against collected experimental data. Problems with defining well posed

---

**1 Introduction**

Fluid flow and thermal effects during melting and solidification are of great interest in a number of manufacturing processes, where a solid material is formed by the freezing of a liquid. Its main characteristic is that a moving interface separates two phases with different physical properties. Temperature differences in the melt give rise to buoyancy forces that produce significant convective flow. It appears that there is a close relationship between the structure of the solid

initial conditions, effects of supercooling and non-uniformity of the solidus generate additional difficulties in matching experimental data with their numerical counterparts. Nevertheless, our present model seems to offer very promising results, describing most of the observed features of the physical experiment.

## 2 Formulation of the problem

We consider convective flow in a cubic box filled with a viscous heat conducting liquid, which in this case is distilled water. Two opposite vertical walls of the box are assumed isothermal (Fig. 1). One of them is held at temperature  $T_c = -10^\circ\text{C}$ . It is below the freezing temperature of the liquid  $T_r = 0^\circ\text{C}$ , hence the solid forms there. The opposite vertical wall is held at temperature  $T_h = 10^\circ\text{C}$ . The other four walls of low thermal conductivity allow the entry of heat from the environment (air at temperature  $T_{ext} = 25^\circ\text{C}$ ).

For transient processes uncertainty of the initial conditions may create difficulties in matching experimental and numerical results. In any physical experiment small temperature fluctuations inside the fluid, non-uniformity of temperature at the external walls, as well as final rise time for the temperature jump, are inevitable. Hence, to improve our definition of the initial condition, a so called warm start is performed. The freezing starts after the steady convection pattern is established in the cavity. This initial flow state corresponds to natural convection without phase change in the differentially heated cavity, with the temperature of the cold wall set to  $T_c = 0^\circ\text{C}$ . The freezing experiment starts, when at time  $t = 0$ , the cold wall temperature suddenly drops to  $T_c = -10^\circ\text{C}$ . In the numerical runs, the solution obtained for steady state natural convection was used as the initial flow and temperature fields to start the freezing calculations.

The three basic dimensionless parameters describing the problem are: the Rayleigh number ( $Ra$ ), the Prandtl number ( $Pr$ ), and the Stefan number ( $Ste$ ), defined as:

$$Ra = \frac{g\beta\Delta TH^3}{\nu\alpha}, \quad Pr = \frac{\nu}{\alpha}, \quad Ste = \frac{c\Delta T}{L_f}$$

where  $\Delta T = T_h - T_r$  is the difference of the hot wall temperature  $T_h$  and the interface temperature  $T_r$  (melting tem-

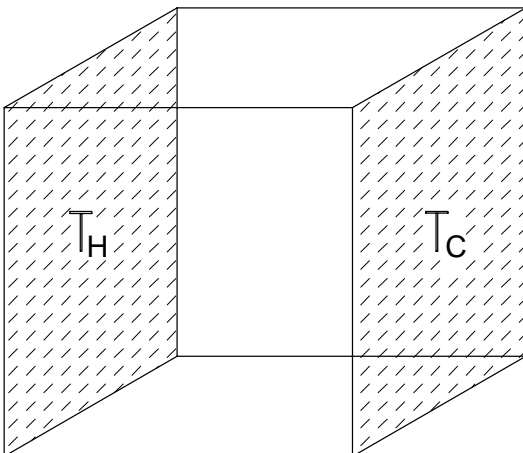


Fig. 1. Physical problem: differentially heated cube shaped cavity

perature). In the above definition  $g$ ,  $H$ ,  $\alpha$ ,  $\beta$ ,  $\nu$ ,  $c$ ,  $L_f$ , denote respectively the gravitational acceleration, the cavity height, the thermal diffusivity, the coefficient of thermal expansion, the kinematic viscosity, the specific heat of fluid and the latent heat of fusion.

Due to the non-linear variation of the water density with temperature the problem is fully prescribed and the use of a non-dimensional description of the problem is only for comparison purposes. The non-dimensional parameters are defined at the arbitrary selected reference temperature  $T_r = 0^\circ\text{C}$ . The corresponding non-dimensional values calculated for a temperature difference  $\Delta T = 10^\circ\text{C}$ , and 38 mm cavity are:  $Ra = 1.503 \cdot 10^6$ ,  $Pr = 13.3$  and  $Ste = 0.125$ .

Non-linear variation of the water density we consider only in the buoyancy term. The water density function used was obtained by fitting a fourth order polynomial to the data collected by Kohlrausch (1968) [15] (fit error 0.02%):

$$\begin{aligned} \rho = & 999.840281167 + 0.0673268037314 \cdot T \\ & - 0.00894484552601 \cdot T^2 \\ & + 8.78462866500 \cdot 10^{-5} \cdot T^3 \\ & - 6.62139792627 \cdot 10^{-7} \cdot T^4 \end{aligned} \quad (1)$$

where the temperature  $T$  is given in degrees Celsius and  $\rho$  in  $\text{kg}/\text{m}^3$ .

The expansion coefficient is obtained by differentiating the above formula:

$$\beta = -\frac{1}{\rho} \frac{d\rho}{dT}$$

Variation with temperature of the remaining physical parameters appeared to have only a secondary effect. Hence, water viscosity  $\nu$ , as well as the thermal conductivity ( $k$ ) and the heat capacity ( $c$ ) of water and ice are assumed to be constant. Their value at the reference temperature  $T_r = 0^\circ\text{C}$  is used:

$$\begin{aligned} \nu &= 1.79 \times 10^{-6} \text{ [m}^2\text{/s]} \\ k_l &= 0.56 \text{ [W/m K]} \\ k_s &= 2.26 \text{ [W/m K]} \\ c &= 4.202 \text{ [kJ/kg K]} \end{aligned}$$

The latent heat is equal  $L_f = 335 \text{ kJ/kg}$ . The thermal conductivity, heat capacity and density of the Plexiglas used were measured. When solving the energy equation for the side walls, the values of  $0.195 \text{ W/mK}$  for the thermal conductivity, and  $1.19 \times 10^{-7} \text{ m}^2\text{/s}$  for the thermal diffusivity were used. The heat transfer coefficient  $h$  used for modelling the convective heat flux from the external fluid was taken to be  $20 \text{ W/m}^2 \text{ K}$ .

## 3 Mathematical model and numerical technique

The numerical study of freezing water has been conducted on a fixed-grid by using a mathematical formulation based on the enthalpy porosity method [6]. One of the advantages of the fixed grid method is that a unique set of equations and boundary conditions is used for the whole domain, including both solid and liquid phase. It allows us to avoid the problem of tracking the solid/liquid interface.

The governing equations are obtained using averaged quantities [7] so the generalised velocity, density, and thermal conductivity are defined as:

$$\begin{aligned} \mathbf{v}_m &= f_s \mathbf{v}_s + f_l \mathbf{v}_l \\ \rho_m &= f_s \rho_s + f_l \rho_l \\ k_m &= g_s k_s + g_l k_l \end{aligned}$$

where  $\mathbf{v}_l$ ,  $\mathbf{v}_s$ , are the velocity of the liquid and solid phase,  $f_l$ ,  $f_s$ , are the liquid and solid mass fraction,  $g_l$ ,  $g_s$  are the liquid and solid volume fraction,  $\rho_l$ ,  $\rho_s$  are the density of the liquid and solid phase. The volume fraction  $g$  is related to the mass fraction  $f_l$  and  $f_s$  via:

$$\begin{aligned} \rho_m f_s &= \rho_s g_s \\ \rho_m f_l &= \rho_l g_l \end{aligned}$$

According to the saturated mixture conditions the mass and volume fractions must add to unity:

$$\begin{aligned} f_s + f_l &= 1 \\ g_s + g_l &= 1 \end{aligned}$$

Using the assumption that the liquid is Newtonian and incompressible, and that the densities ( $\rho$ ) and the specific heat ( $c$ ) in the liquid ( $\cdot$ )<sub>l</sub> and solid ( $\cdot$ )<sub>s</sub> phases are equal and constant, the dimensionless governing equations in a vorticity-velocity formulation are:

$$\frac{\partial \omega_m}{\partial t} + \nabla \times (\omega_m \times \mathbf{v}_m) = Pr \nabla^2 \omega_m - \quad (2)$$

$$Ra Pr \sum_{i=1}^N \gamma_i \theta^i \left( \frac{\mathbf{g}}{|g|} \right) + \nabla \times \mathbf{S} \quad (3)$$

$$\nabla^2 \mathbf{v}_m = -\nabla \times \omega_m \quad (4)$$

$$\frac{\partial \theta}{\partial t} + (\mathbf{v}_m \cdot \nabla) \theta = \nabla \cdot (\tilde{k} \nabla \theta) + B \quad (4)$$

where:

$$\gamma_i = \frac{a_i}{a_1} \Delta T^{(i-1)}$$

and  $a_i$  are the coefficients in the density expression (1) and  $\Delta T = T_h - T_r$  is the temperature difference of the hot wall  $T_h$  and the phase interface temperature  $T_r$ . The dimensionless conductivity is defined as:

$$\tilde{k} = (1 - f_l) \frac{k_s}{k_l} + f_l$$

In this way, in the liquid zone ( $f_l = 1$ )  $\tilde{k} = 1$ , and in the solid zone ( $f_l = 0$ )  $\tilde{k} = \frac{k_s}{k_l}$ .

A modified Boussinesq approximation has been used, that is the non linear density variation has been considered only in the buoyancy term.

The Darcy type [7] source term has been adopted in the momentum equation to gradually reduces velocity in the solidifying zone:

$$\mathbf{S} = \frac{-C(1 - f_l)^2}{(f_l^3 + q)} \mathbf{v}_m$$

Where  $C$  is a large constant value and  $q$  is a computational small quantity used to avoid singularity in solid zone ( $\approx 10^{-3}$ ).

In the energy equation (4) the last term at the right-side is given by

$$B = -\frac{1}{Ste} \frac{\partial f_l}{\partial t}$$

which takes into account the latent heat due to phase change.

The governing equation eq. (2–4) are discretised using a finite volume technique on a staggered grid. A fully implicit method has been adopted for the mass and momentum equations, while the temperature field is solved separately in order to evaluate the variation in the local liquid phase fraction. The two linearised algebraic systems are solved using a preconditioner BI-CGStab method [8].

At each time step the liquid fraction and the temperature field in (4) are solved by using an iterative procedure. At the time step  $n + 1$  the initial iterative fields are initialised to previous time step  $n$  then the following iterative system eqs. (5–7) is solved:

$$f_l^i = f_l^{i-1} + Ste (\theta^{i-1} - \theta_s) \quad (5)$$

Subject to the following constraint:

$$f_l^i = \max [0, \min (f_l^i, 1)] \quad (6)$$

$$Ste \left( \frac{\theta^i - \theta^n}{\Delta t} \right) + Ste \nabla \cdot (\mathbf{v}_m^n \theta^i) = Ste \nabla \cdot (\tilde{k} \nabla \theta^i) + \frac{f_l^n - f_l^i}{\Delta t} \quad (7)$$

where  $i$  is the index of the iteration level,  $\Delta t$  the time step discretization and  $\theta_s$  the phase change temperature. The steps (5–7) are repeated until

$$\|f_l^i - f_l^{i-1}\| < \varepsilon_1 \text{ and } \|\theta^i - \theta^{i-1}\| < \varepsilon_2$$

and typically  $\varepsilon_1 = \varepsilon_2 = 10^{-8}$  was used.

## 4 Experimental

Our main interest is directed collecting quantitative information about the phase front position as well as about velocity and temperature fields within a domain of a mid-height vertical plane of the cavity. For this purpose the flow images of the centre vertical cross-section have been collected periodically every 60 s or 120 s, for approximately two hours from the onset of cooling. At each time step a series of three to ten RGB images are taken at a short time interval. Special acquisition and image analysis software has been developed and used to obtain 2-D flow pattern (particle tracks) and temperature and velocity fields ([9–11]).

### Apparatus

The experimental set-up used to acquire temperature and velocity fields consists of the convection box, a light source, a 3CCD colour camera (KYF55 JVC). The flow field was illuminated with a 2 mm thin sheet of white light from a specially

constructed halogen lamp, and observed at the perpendicular direction. The 24-bit colour images of  $560 \times 560$  pixels were acquired using a 32-bit PCI bus frame grabber (AM-STD-RGB Imaging Technology Inc.). The convection box, of 38 mm inner dimension, has two isothermal walls made of aluminium. The four non-isothermal walls were made of 6 mm thick Plexiglas. The isothermal walls were maintained at a constant temperature by anti-freeze coolant flowing through the attached antechamber. Thermostats controlled the temperature of the cooling and heating liquids. The freezing experiment starts by opening abruptly the inlet valves to the coolant passages. The temperature of the cold and hot wall was  $-10^\circ\text{C}$  and  $+10^\circ\text{C}$ , respectively. Distillate water was selected as a flow medium for its well known thermophysical properties and well defined temperature of the phase change.

#### *Velocity and temperature measurements*

Both velocity and temperature fields were monitored using unencapsulated Thermochromic Liquid Crystal (TLC) tracers ([4, 12]). Digital evaluation of tracer images collected for the selected flow cross-section (Digital Particle Image Velocimetry and Thermometry) allows us simultaneous and fully automatic measurements of temperature and velocity 2-D flow fields. Temperature is determined by relating colour of the tracers to a temperature calibration function ([11, 13]). The 2-D velocity vector distribution has been measured by digital particle image velocimetry (DPIV). For this purpose, the colour images of TLC tracers are transformed to B&W intensity images. The magnitude and direction of the velocity vectors are determined using the recently developed evaluation technique based on the Optical Flow approach [14].

To get a general view of the flow pattern, several images recorded periodically within a given time interval have been added in the computer memory. Displayed images are similar to the multiexposed photographs, showing the flow direction and its structure (see Fig. 2a). This type of visualization is very effective in detecting small re-circulation regions, usually difficult to identify in the velocity field. In all cases studied the volume concentration of tracers was very low (below 0.1%), so their effect on the flow and the physical properties of water was negligibly small.

The flow images are used to evaluate the shape and location of the phase front. These measurements are performed manually using image analysis software. The accuracy of a single point measurement is about 1 pixel, which corresponds to 0.07 mm.

## 5 Selected results

### *Natural convection*

At the beginning, our interest was directed to verify numerical solutions obtained for natural convection of water in the vicinity of the freezing point. In the experiments the cold wall temperature was set to  $0^\circ\text{C}$ , and the hot wall to  $+10^\circ\text{C}$ . The effects of density inversion and of the thermal boundary conditions at non-isothermal walls on the flow structures are studied to compare and eventually improve the numerical code.

A typical flow structure (see Fig. 2) exhibits two recirculation regions, upper one, where the water density decreases with temperature, and the lower region with an abnormal density variation. Similar flow patterns were obtained in the numerical solution (Fig. 3, 4), however several discrepancies are present. Numerical experimentation with thermal boundary conditions posed at the non-isothermal walls has shown that the calculated flow pattern strongly depends on the modelling used. Small changes of the heat flux through these passive walls evidently shifts the saddle point (Table 1) present at the cold wall, modifying the size of both flow circulations. Figure 5 illustrates variation of the vertical vorticity profiles along the cold wall calculated for different heat fluxes through the side walls.

It was concluded, that neither isothermal or constant heat flux models are sufficiently accurate to obtain observed flow structures. The observed flow configuration, with two interacting cold and warm counter-rotating circulation, appears to be very sensitive to changes of the heat flux through side walls. Hence, direct comparison of the numerical and experimental results is necessary to verify assumptions made for heat transfer coefficients at the external surfaces. Solving the coupled solid-fluid heat conduction problem together with the Navier-Stokes equations evidently improved the modelling of

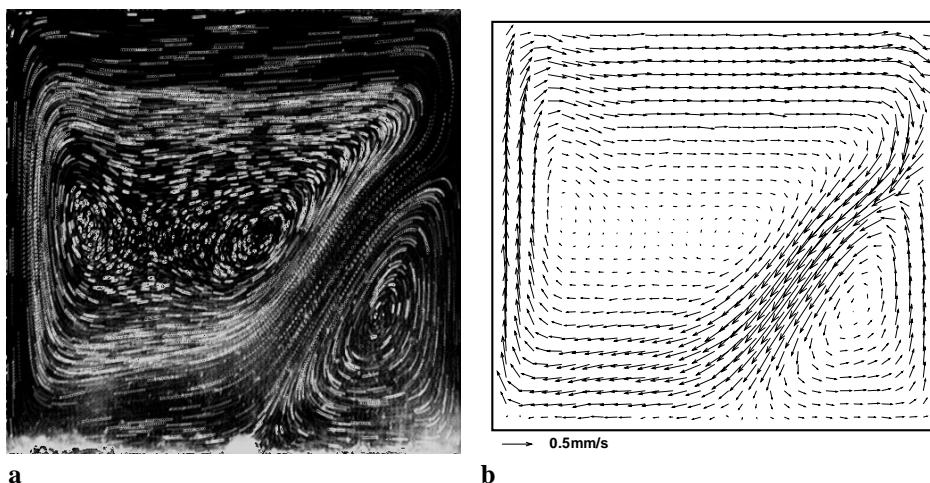
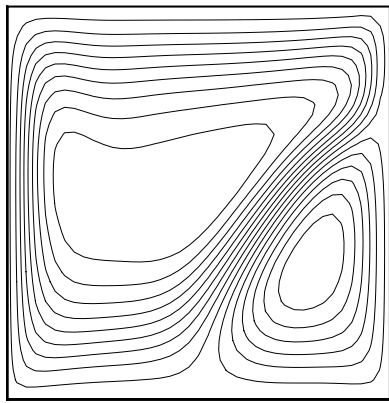
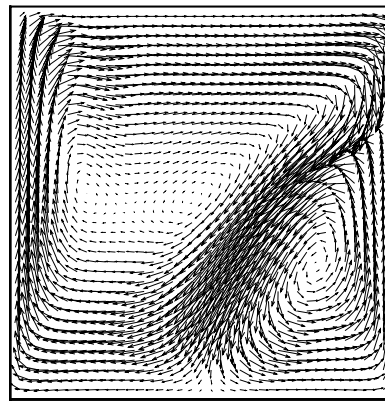


**Fig. 2a,b.** Natural convection of water observed for  $T_h = 10^\circ\text{C}$ ,  $T_c = 0^\circ\text{C}$ . **a** Flow pattern visualized on multiexposed image of traces; **b** Evaluated velocity field using PIV technique

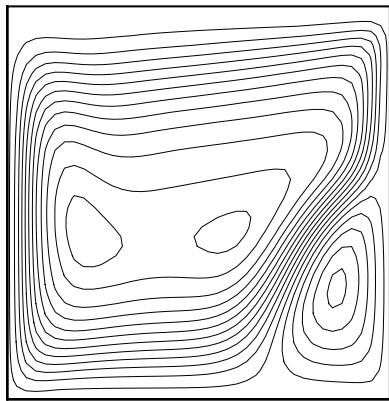


a

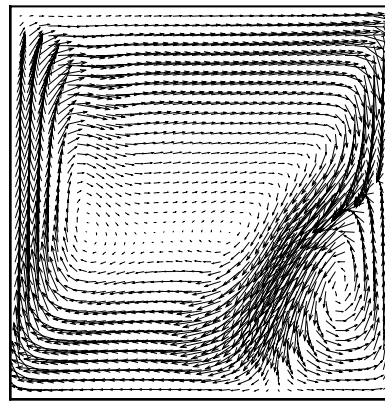


b

Fig. 3a,b. Natural convection of water for  $T_h = 10^\circ\text{C}$ ,  $T_c = 0^\circ\text{C}$ , flow field calculated for adiabatic boundary conditions. a Stream function; b Velocity vectors



a



b

Fig. 4a,b. Natural convection of water for  $T_h = 10^\circ\text{C}$ ,  $T_c = 0^\circ\text{C}$ , flow field calculated for conducting walls solving the conjugate heat transfer problem. a Stream function; b Velocity vectors

Table 1. Saddle point position

Numerical adiabatic walls	Numerical conducting walls	Experimental
0.714	0.585	0.625

the flow pattern, but still empirical values for the air-wall heat flux coefficients have to be used.

*Freezing of water*

The pure convection experiments show as already mentioned two main flow circulation regions. In the first, driven by normal convection and located in the upper part of the cavity, there is a clockwise circulation. It transports the hot liquid up to the top wall and back along the isotherm of the density extreme. When freezing starts from developed flow, the thermal boundary conditions at the cold side remain the same, i.e. isothermal surface at temperature  $0^\circ\text{C}$ . However, interaction of the convective flow with the freezing front causes deformation of initially flat freezing plane. The hot circulation melts the upper parts of the ice front, reducing the ice growth rate in this region. The abnormal flow circulation, located in the lower right part of the cavity, transports the cold liquid up along the adjacent ice surface and back to the bottom along the isotherm of the density extremum. This cold

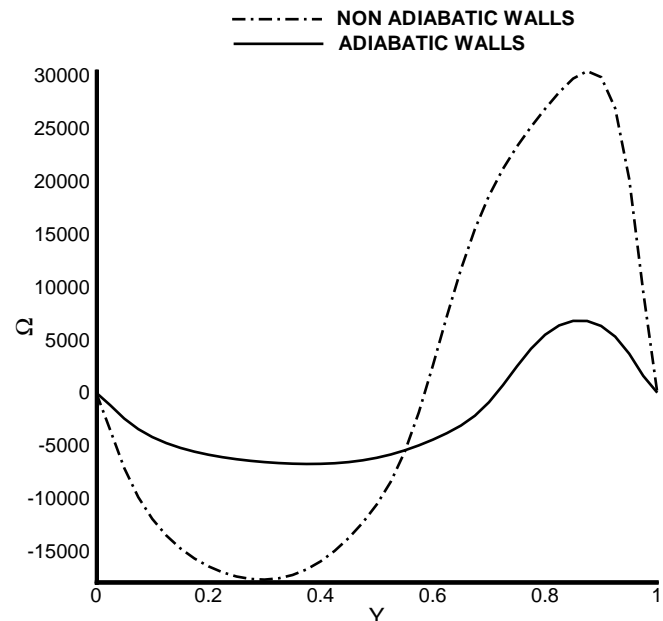
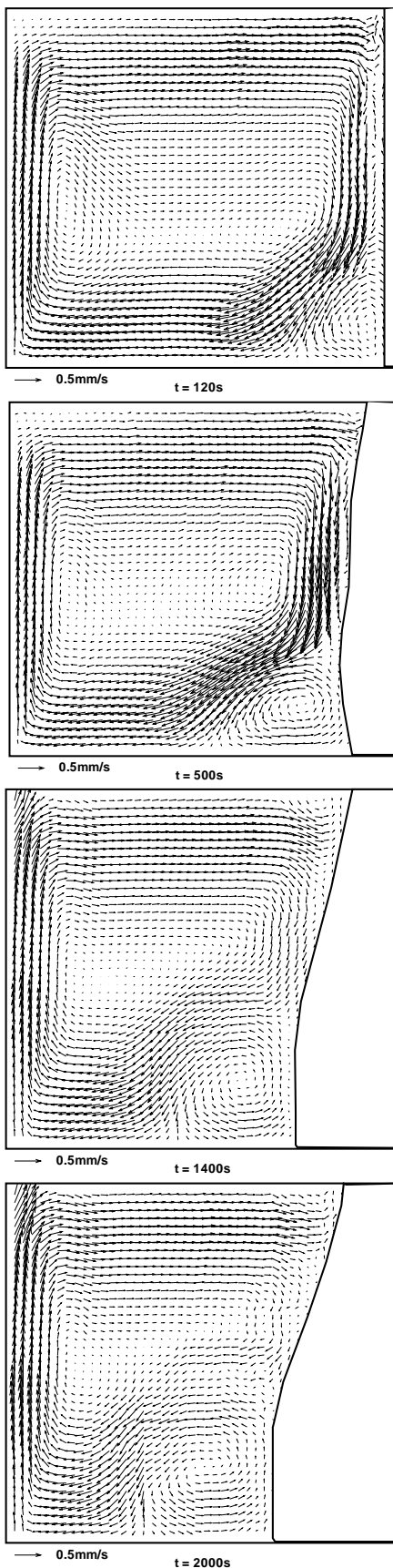


Fig. 5. Vertical vorticity profiles extracted along the cold wall. The strong dependence of the saddle point position (zero crossing of the profile) on heat flux through the side walls is shown

water circulation only moderately modifies the heat balance at the interface. The convective heat transfer between both upper and lower regions seems to be limited mainly to the upper



**Fig. 6.** Measured velocity field at 120 s, 500 s, 1400 s, and 2000 s after freezing process starts from the steady convective flow;  $T_h = 10^\circ\text{C}$ ,  $T_c = -10^\circ\text{C}$

right corner of the cavity. There, along the colliding cold and warm fluid layers, the heat is transferred from the hot wall to the lower parts of the cavity. The shape of the freezing front reproduces this interaction, almost doubling the ice growth rate at the bottom (see Fig. 6).

Comparison of the measured and calculated (see Fig. 7) ice fronts indicates qualitative agreement. For short time (first 500 s), there is also quite good quantitative agreement between simulated and experimental results. However, with progressive development of the solidus differences of the front shape appear to grow. Especially lower parts of the ice front suffer evident errors in modelling. Numerical counter-clockwise circulation at the lower parts seems to be more effective in decreasing ice growth. In the experiments the ice surface remains almost perpendicular to the bottom wall, whereas in the numerical results for large time its shape declines strongly back into the cold wall.

## 6 Discussion

The results obtained show a very good agreement between numerical and experimental results for initial time of this transient process. The agreement progressively decreases for longer experimental time. One of our future aims is to improve the capacity of the prediction of the numerical model for long simulation times. Since at longer times the ice layer is quite thick, it seems important to improve modelling of thermal conductivity inside the solid. Non-uniformity of the ice structure, dendrites, and impurities due to the solved gases may force us to verify the assumption used about isotropy of the thermal properties of the ice.

Another important point is analysis of the effects of supercooling. As a matter of fact, most of the investigations concerning solidification assume the isothermal conditions at the phase change boundary and the temperatures above the freezing point for the liquid phase. However, it is well known that usually the fluid supercooling precedes the phase change [16]. For example, we observed in the experiments that water of standard purity will supercool to about  $-5^\circ\text{C}$  to  $-7^\circ\text{C}$ , before ice nucleation appears. This may significantly retard the solidification process, modifying initial flow pattern. Thus, an understanding of the role of supercooling in the solidification process seems to be worthwhile. The accurate modelling of the supercooling is not straightforward. The supercooling depends on concentration of the nucleation sites, the cooling rate and the cooling history. Theoretical prediction of these parameters is rather imprecise. Our experiments with freezing water indicate that in most of the cases distilled water cools to about  $-7^\circ\text{C}$  before phase change begins. The observed effect of supercooling qualitatively changes the onset of freezing. The proper definition of the initial flow conditions for the numerical simulation becomes controversial. Modelling of supercooling for the formation of ice was not present in the numerical model. However, we believe this is important and is part of work being undertaken.

*Acknowledgements.* We gratefully acknowledge CIRA S.c.p.A. (Centro Italiano Ricerche Aerospaziali) for the use of the POWER CHALLENGE supercomputer. The third author acknowledge research grant of KBN (State Committee for Scientific Research).

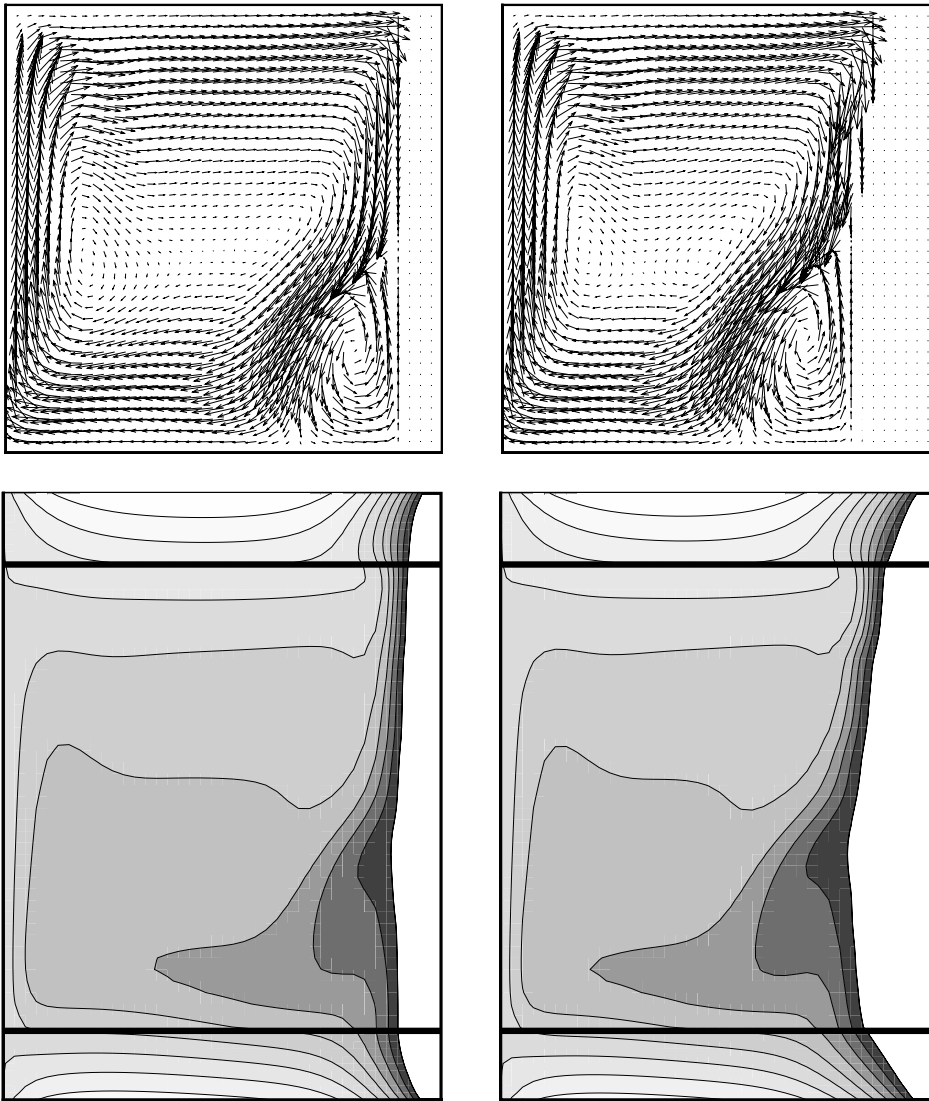


**Fig. 7.** Freezing of water:  $T_h = 10^\circ\text{C}$ ,  $T_c = -10^\circ\text{C}$ . Numerical solutions obtained at 120 s (left column) and 500 s (right) after freezing starts from the steady convective flow. Velocity vectors (top row) and temperature fields (bottom) displayed

## References

1. Yeoh, G.H., Behnia, M., de Vahl Davis, G., Leonardi, E.: A numerical study of three-dimensional natural convection during freezing of water. *Int. J. Num. Meth. Eng.* 30, 899–914 (1990)
2. Banaszek, J., Rebow, M., Kowalewski, T.A.: Fixed grid finite element analysis of solidification. In: *Adv. in Computational Heat Transfer. CHT-97.* 471–478. Begel House Inc.: New York 1998
3. Giangi, M., Stella, F., Kowalewski, T.A.: Numerical simulation of natural convection during ice formation. IV Congresso nazionale della società italiana di matematica applicata ed industriale. (Simai) 1–5 giugno 1998
4. Kowalewski, T.A., Rebow, M.: An experimental benchmark for freezing water in the cubic cavity. *Advances in Computational Heat Transfer CHT-97.* p. 149–156. Begel House Inc.: New York 1998
5. Kowalewski, T.A.: Experimental validation of numerical codes in thermally driven flows. *Advances in Computational Heat Transfer CHT-97.* p. 1–15. Begel House Inc.: New York 1998
6. Voller, V.R., Cross, M., Markatos, N.C.: An enthalpy method for convection-diffusion phase change. *Int. J. Num. Meth. Eng.* 24, 271–284 (1987)
7. Slatery, J.C.: *Momentum energy and mass transfer in continua.* Kieger: New York 1987
8. Van De Worst, H.: A fast and smoothly converging variant of Bi-Cgstab for the solution of non-symmetric linear systems. *SIAM J. Sci. Stat. Comput.* 132, 631–644 (1992)
9. Hiller, W.J., Koch, S., Kowalewski, T.A., Stella, F.: Onset of natural convection in a cube. *Int. J. Heat Mass Transfer.* 36, 3251–3263 (1993)
10. Abegg, C., de Vahl Davis, G., Hiller, W.J., Koch, S., Kowalewski, T.A., Leonardi, E., Yeoh, G.H.: Experimental and numerical study of three-dimensional natural convection and freezing in water. *Heat Transfer.* 4, 1–6. IchemE, Taylor & Francis: London 1994
11. Kowalewski, T.A., Cybulski, A.: Experimental and numerical investigations of natural convection in freezing water. *Int. Conf. on Heat Transfer with Change of Phase.* Kielce, in *Mechanics.* 61(2), 7–16 (1996)
12. Kowalewski, T.A., Rebow, M.: Freezing of water in the differentially heated cubic cavity. *Int. J. of Comp. Fluid Dyn.* 11, 193–210 (1999)
13. Kowalewski, T.A., Cybulski, A.: Natural convection with phase change (in polish). IPPT Reports 8/1997. IPPT PAN: Warszawa 1997
14. Quenot, G., Pakleza, J., Kowalewski, T.A.: Particle Image Velocimetry with Optical Flow. *Experiments in Fluids* 25, 177–189 (1998)
15. Kohlrausch, F.: *Praktische Physik.* Band 3. 22. Auflage, Table 22203. pp. 1692–1693. B.G. Teubner: Stuttgart 1968
16. Knight, C.A.: *The freezing of supercooled liquids.* D. Van Nostrand Co: Toronto 1967
17. Gau, C., Viskanta, R.: Flow visualization during solid-liquid phase change heat transfer: Freezing in a rectangular cavity. *Int. Commun. Heat Mass Transfer* 10, 173–181 (1983)
18. Lin, D. S., Nansteel, M.W.: Natural convection heat transfer in a square enclosure containing water near its density maximum. *Int. J. Heat Mass Transfer* 30, 2319–2329 (1987)

19. Mallinson, G.D., de Vahl Davis, G.: Three-dimensional natural convection in a box: a numerical study. *J. Fluid Mech.* 83, 1–31 (1977)
20. Ramachandran, N., Gupta, J.P., Jaluria, Y.: Thermal and fluid flow effects during solidification in a rectangular enclosure. *Int. J. Heat Mass Transfer* 25, 187–194 (1982)
21. Reizes, J.A., Leonardi, E., de Vahl Davis, G.: Natural convection near the density extremum of water. *Proc. of Fourth Int. Conf. on Numerical Methods in Laminar and Turbulent Flow.* pp. 794–804. Swansea: U.K. 1985
22. Robillard, L., Vasseur, P.: Transient natural convection heat transfer of water with maximum density effect and supercooling. *Trans. ASME* 103, 528–534 (1981)
23. Viswanath, R., Jaluria, Y.: A comparison of different solution methodologies for melting and solidification problems in enclosures. *Num. Heat Transfer B* 24, 77–105 (1993)
24. Yeoh, G.H.: Natural convection in a solidifying liquid. Ph.D. Thesis. The University of New South Wales, 1993